Published in final edited form as:
Clin Cancer Res. 2009 December 1; 15(23): 7266–7276. doi:10.1158/1078-0432.CCR-09-1665.

Inhibition of mTOR is required for optimal antitumor effect of HER2 inhibitors against HER2-overexpressing cancer cells

Todd W. Miller[1], **James T. Forbes**[1], **Chirayu Shah**[2,3], **Shelby K. Wyatt**[2,3], **H. Charles Manning**[2,6,10], **Maria G. Olivares**[7], **Violeta Sanchez**[1], **Teresa C. Dugger**[1], **Nara de Matos Granja**[7], **Archana Narasanna**[1], **Rebecca S. Cook**[8,10], **J. Phillip Kennedy**[9], **Craig W. Lindsley**[9], and **Carlos L. Arteaga**[1,8,10]

[1]Department of Medicine, Vanderbilt-Ingram Comprehensive Cancer Center, Vanderbilt University, Nashville, TN

[2]Department of Radiology and Radiological Sciences, Vanderbilt-Ingram Comprehensive Cancer Center, Vanderbilt University, Nashville, TN

[3]Vanderbilt University Institute of Imaging Science, Vanderbilt-Ingram Comprehensive Cancer Center, Vanderbilt University, Nashville, TN

[4]Department of Biomedical Engineering, Vanderbilt-Ingram Comprehensive Cancer Center, Vanderbilt University, Nashville, TN

[5]Department of Neurosurgery, Vanderbilt-Ingram Comprehensive Cancer Center, Vanderbilt University, Nashville, TN

[6]Program in Chemical and Physical Biology, Vanderbilt-Ingram Comprehensive Cancer Center, Vanderbilt University, Nashville, TN

[7]Department of Pathology, Vanderbilt-Ingram Comprehensive Cancer Center, Vanderbilt University, Nashville, TN

[8]Department of Cancer Biology, Vanderbilt-Ingram Comprehensive Cancer Center, Vanderbilt University, Nashville, TN

[9]Department of Chemistry, Vanderbilt-Ingram Comprehensive Cancer Center, Vanderbilt University, Nashville, TN

[10]Breast Cancer Research Program, Vanderbilt-Ingram Comprehensive Cancer Center, Vanderbilt University, Nashville, TN

Abstract

Purpose—A significant fraction of HER2-overexpressing breast cancers exhibit resistance to the HER2 antibody trastuzumab. Hyperactivity of the phosphatidylinositol-3 kinase (PI3K)/AKT pathway confers trastuzumab resistance, and mTOR is a major downstream effector of PI3K/AKT. Therefore, we examined whether mTOR inhibitors synergize with trastuzumab.

Experimental Design—Immunocompetent mice bearing HER2-positive mammary tumors were treated with trastuzumab, the mTOR inhibitor rapamycin, or the combination. Mice were imaged for tumor cell death using an optical Annexin-V probe and with [^{18}F]FDG-PET. The signaling and growth effects of the mTOR inhibitor RAD001 on HER2+ cells treated with trastuzumab or lapatinib were evaluated.

To whom reprint requests should be sent: Carlos Arteaga 2200 Pierce Avenue, 777 PRB Vanderbilt University Medical Center Nashville, TN 37232-6307 carlos.arteaga@vanderbilt.edu.

Results—Treatment of mice with trastuzumab plus rapamycin was more effective than single-agent treatments, inducing complete regression of 26/26 tumors. The combination induced tumor cell death (Annexin-V binding) and inhibited FDG uptake. Rapamycin inhibited mTOR and tumor cell proliferation as determined by phospho-S6 and Ki67 immunohistochemistry, respectively. In culture, the combination of RAD001 plus trastuzumab inhibited cell growth more effectively than either drug alone. Trastuzumab partially decreased PI3K but not mTOR activity. Knockdown of *TSC2* resulted in HER2-independent activation of mTOR and dampened the response to trastuzumab and lapatinib. Treatment with the HER2 inhibitor lapatinib decreased phospho-S6 and growth in *TSC2*-expressing but not in *TSC2*-knockdown cells.

Conclusions—Inhibition of PI3K and mTOR are required for the growth inhibitory effect of HER2 antagonists. These findings collectively support the combined use of trastuzumab and mTOR inhibitors for the treatment of HER2+ breast cancer.

Keywords

mTOR; trastuzumab; HER2; breast cancer

Introduction

Amplification and/or overexpression of the *HER2/erbB2* oncogene occurs in 20-30% of human breast cancers and is associated with poor prognosis (1,2). The humanized monoclonal antibody trastuzumab (Tz, Herceptin®), which binds the extracellular region of human HER2 (3), is approved for the treatment of HER2+ breast cancer. Adjuvant Tz therapy significantly improves patient outcome overall. However, in the metastatic setting, only a fraction of patients with HER2+ disease responded to Tz therapy (4-8), implying that many advanced cancers are Tz-resistant. HER2+ breast tumors showed increased caspase-3 activation following one week of neoadjuvant Tz treatment (9), indicative of apoptosis. Although the anti-tumor mechanism (s) of Tz action remains unclear, the immunologic effects of this antibody are thought to be critical, likely invoking antibody-dependent cellular cytotoxicity (10).

HER2 dimerizes with members of the epidermal growth factor receptor tyrosine kinase family (EGFR, HER3, HER4) to induce downstream signaling cascades. The most oncogenic heterodimer is HER2/HER3, which engages downstream signaling pathways including phosphatidylinositol-3 kinase (PI3K)/AKT. Tz induces a cytostatic effect on HER2+ breast cancer cell lines in culture (11) correlating with partial inhibition of AKT activation (12). However, HER2+ primary breast tumors did not exhibit significant Tz-induced downregulation of phosphorylated AKT (P-AKT) or P-Erk (9), suggesting that Tz is not a potent inhibitor of HER2 signaling *in vivo*.

Mutational activation of the PI3K pathway by activating mutations in *PIK3CA* (encoding the PI3K p110α catalytic subunit) or loss-of-function mutations in *PTEN* (encoding a lipid phosphatase that antagonizes PI3K) has been linked to Tz resistance in cancer cells and primary tumors (13,14). We reported that HER2+ BT474 human breast cancer cells selected for Tz resistance *in vivo* maintained PI3K activity and were sensitive to pharmacological inhibitors of receptors upstream of PI3K (15). Tz inhibits PI3K signaling in parental but not Tz-resistant BT474 cells, suggesting that these cells escape Tz action through PI3K activation (15).

The mTORC1 complex (hereafter referred to as mTOR) is a major downstream effector in the PI3K/AKT pathway (16). Additionally, mTOR may be modulated by an AKT-independent mechanism via protein kinase C (17). mTOR inhibitors [e.g., rapamycin, RAD001 (everolimus)] are being tested clinically for the treatment of breast and other cancers (18,19). Rapamycin blocked PTEN-deficient tumor formation in mice (20). mTOR inhibitors block cancer cell proliferation in culture (21,22), and decrease tumor angiogenesis and vessel

permeability *in vivo* (23). Results of phase I trials in patients with Tz-resistant (24) and heavily pretreated (25) breast cancers have shown that the combination of RAD001 and Tz may be a promising treatment option. We speculated that the inability of Tz to completely block PI3K/AKT/mTOR signaling would permit synergy of Tz with mTOR inhibitors to suppress the growth of HER2+ cancer cells. Additionally, mTOR inhibitors may have effects on host (non-tumor) cells that contribute to their synergy with Tz.

Materials and Methods

Tumor studies

Female mice expressing a MMTV promoter-driven human *HER2* transgene develop mammary gland tumors (26). Tumors were harvested from MMTV/HER2 females [gift from Sharon Erickson, Genentech]. Two-mm pieces were transplanted subcutaneously near mammary gland #1 of syngeneic wild-type FVB females (5-7 weeks old) as described (27). Palpable tumors arose after 4-8 weeks. Tumors were measured 2x/week, and volume was calculated as $width^2 \times length/2$. To account for the variability in response to drug treatment seen in this model (26,27), transplanted tumors were derived from a different transgenic donor for each experiment. Tumor-bearing mice were randomized to treatment with vehicle(s), Tz (30 mg/kg in PBS, administered i.p. 2x/week; Vanderbilt University Hospital Pharmacy), rapamycin (1 mg/kg in 5% PEG-400/5% Tween-80/0.9% NaCl, administered i.p. 3x/week; Eton Biosciences), or the combination. Mouse studies were approved by the Vanderbilt IACUC.

Immunohistochemistry

Formalin-fixed tumors were paraffin-embedded. Five-μm sections were used for H&E staining, and IHC using antibodies against Ki67 (Biocompare), P-$HER2_{Y1248}$ (scoring described in Supplementary Methods), P-$S6_{S235/236}$, and P-AKT_{S473} (Cell Signaling). Ki67 was scored as % positively-stained cells in 10 fields (400x magnification) of viable tumor. P-S6 and P-AKT staining were evaluated by an expert pathologist (M.G.O.) as described (28).

Cell proliferation

BT474 and SKBR3 cells (ATCC) were maintained in IMEM/10% FBS and McCoy's 5A medium/15% FBS (Gibco), respectively. HR5 and HR6 cells were maintained in IMEM/10% FBS plus 10 μg/mL Tz as described (15). Cells were seeded in triplicate (4×10^4/well, 12-well plates), then treated ± Tz (21 μg/mL), RAD001 [20 nM, gift from Carlos Garcia-Echeverria, Novartis (29)], 0360263-1 [AKTi, 1 μm, AKT1/2 inhibitor (30)], lapatinib ditosylate (1 μM, GW-572016, LC Laboratories), or combinations. For siRNA experiments, cells were transfected with siRNA targeting *TSC2* (Qiagen cat. #SI00011697) or non-silencing control (Qiagen, cat. #1027280), and then reseeded for cell proliferation assays and immunoblotting. Media plus drugs were replenished every 2-3 days, and cells were trypsinized and counted using a Coulter counter after 6-7 days.

Immunoblotting

Cells and tumor samples were lysed in 1% NP-40 buffer containing protease and phosphatase inhibitors. Samples were sonicated for 10 sec., centrifuged at 14,000 rpm for 5 min., and protein concentrations quantitated using BCA assay (Pierce). Lysates were used for immunoblotting with S6, P-$S6_{S235/236}$, AKT, P-AKT_{S473}, P-AKT_{T308}, P-MAPK, MAPK, P-$HER3_{Y1289}$, P-$EGFR_{Y1173}$, P-$HER2_{Y1248}$ (Cell Signaling), HER3 (Santa Cruz), HER2 (Neomarkers), and actin (Sigma) antibodies.

In vivo imaging

Mice were imaged using NIR700-Annexin-V (details provided in Supplementary Methods) at baseline (pretreatment) when tumor size reached ≥400 mm^3, then randomized to treatment with Tz, rapamycin, or the combination, and re-imaged 40 h later. Differences between pre- and post-treatment absolute tumor fluorescence (ATF) were calculated. Mice were imaged using [^{18}F]FDG-PET at baseline, then randomized to drug treatment on days 0, 2, 4, and 6, and reimaged on days 3 and 7. Percent changes in [^{18}F]FDG tumor uptake comparing pre- vs. post-treatment were calculated.

Statistics

Mann-Whitney U-test was used to determine the significance of differences between groups in tumor volumes, % Ki67+ cells, NIR700-Annexin-V and [^{18}F]FDG uptake. *T*-testing was used to determine the significance of changes in cell proliferation. $p<0.05$ was considered significant.

Results

Rapamycin in combination with trastuzumab induces complete regression of MMTV/HER2 tumors

We transplanted tumors from three MMTV/HER2 transgenic female mice into three groups of 30 wild-type female mice each (referred to as groups A, B, and C). Tumor-bearing mice were randomized to treatment with Tz or PBS once tumor volumes reached ≥200 mm^3. While tumor volume continued to increase in PBS-treated mice, Tz treatment inhibited tumor growth in all three groups (Fig. 1). In groups A and C, Tz treatment for three weeks induced complete tumor regression in 7/10 and 6/8 mice, respectively (Figs. 1A, 1C, S1). While Tz treatment significantly slowed the growth of group B tumors (Fig. 1B), 9/10 group B tumors continued to grow during Tz therapy, and 25-30% of tumors in groups A and C grew or did not regress completely even after four weeks, suggesting that a fraction of MMTV/HER2 tumors are Tz-resistant. In agreement with prior findings in MMTV/HER2 tumors (26), tumors from groups A-C showed strong HER2 immunoreactivity by IHC (not shown), and Tz treatment did not alter P-HER2Y1248 immunoreactivity (Fig. S1D).

We next determined whether co-treatment with the mTOR inhibitor rapamycin synergizes with Tz to inhibit MMTV/HER2 tumor growth. We previously found that larger MMTV/HER2 tumors were less sensitive to Tz therapy (27), so we allowed group D tumors to grow to ≥400 mm^3 before initiating treatment. Treatment with Tz or rapamycin alone significantly inhibited tumor growth to similar extents compared to vehicle control (Fig. 2A-B, all $p<0.05$); four weeks of single-agent treatments induced complete regression in only 3/10 and 1/10 cases, respectively. In contrast, the combination treatment significantly decreased tumor volume within 0.5 weeks compared to baseline ($p<0.005$), induced complete regression in all cases within 3.5 weeks, and was significantly more inhibitory than either drug alone (Tz vs. combination $p<0.05$ at 1 week and thereafter; rapamycin vs. combination $p<0.001$ at 1.5 weeks and thereafter). The treatment combination also more effectively inhibited tumor growth and induced complete regression than either drug alone when initiated with tumors ≥200 mm^3 (Fig. 2C-D).

Treatment with rapamycin decreases tumor cell proliferation and mTOR activity

To determine the effects of these treatments on tumor cell proliferation and survival, we randomized mice bearing tumors ≥400 mm^3 to Tz, rapamycin, or the combination. Mice were treated on days 0 and 2, and tumors were harvested 24 hours later on day 3. Immunohistochemical analysis showed that the percentage of Ki67+ tumor cells decreased

upon treatment with rapamycin alone (1.8 ± 1.7%, average ± SEM) or in combination with Tz (2.6 ± 1.7%), while Tz alone (20 ± 11.5%) had no significant effect on the proportion of Ki67 + cells compared to controls (24.3 ± 9.8%; Fig. 3A-B; $p<0.0005$). This suggests that rapamycin suppressed cell proliferation, and confirms previous observations that Tz does not alter tumor cell proliferation *in vivo* (9, 31). Immunohistochemical analysis of cleaved caspase-3 in tumors harvested after three and six days of treatment showed apoptosis surrounding prominent necrotic regions, but we did not detect differences in caspase-3 immunoreactivity or the extent of areas of necrosis between treatment groups (not shown). However, we recently showed that two weeks of Tz treatment induces apoptosis in MMTV/HER2 tumors when assessed by optical imaging (31). We speculate that the difference in timing and the large areas of necrosis observed herein may have obscured effects of Tz on apoptosis as measured previously by cleaved caspase-3 IHC in clinical specimens (9). Although mTOR inhibitors may have anti-angiogenic effects (23), CD31 staining did not reveal changes in blood vessel number, size, or architecture between treatment groups (not shown).

We next assessed the effects of Tz and rapamycin on HER2 and mTOR signaling. Rapamycin alone or with Tz effectively blocked S6 ribosomal protein phosphorylation (P-S6) as measured by IHC of tumor sections or by immunoblot of tumor homogenates (Fig. 3A,C), consistent with inhibition of mTOR and its downstream target S6 kinase (32). Tz did not decrease P-S6, modestly decreased P-HER3, but did not alter P-AKT, P-MAPK, P-HER2, or HER2. P-AKT immunoreactivity was not altered by drug treatment (Fig. S2). These results suggest that rapamycin, but not Tz, blocks mTOR activity *in vivo*.

Trastuzumab plus rapamycin treatment decreases tumor viability and glucose metabolism

We next determined the effects of treatment on the induction of cell death by *in vivo* imaging using NIR-labeled Annexin-V, a 35-kDa phosphatidylserine (PS)-binding protein. PS is externalized to the outer leaflet of the plasma membrane during programmed cell death. We previously demonstrated that NIR700-Annexin-V detects apoptosis in MMTV/HER2 tumors after two weeks of Tz treatment (31).

Mice bearing MMTV/HER2 tumors were imaged using NIR700-Annexin-V to establish baseline tumor uptake (Fig. 4A). Mice were then randomized to a single treatment with Tz, rapamycin, or the combination, and re-imaged 40 h later. The changes in absolute tumor fluorescence induced by drug treatment were plotted (Fig. 4A). Single-agent treatments did not alter tumor NIR700-Annexin-V uptake compared to controls, but the combination significantly increased absolute tumor fluorescence ($p<0.05$), suggesting that tumor cell death occurs within 1.5 days of combination treatment. These results contrast with the data obtained with cleaved caspase-3 IHC and suggest this last method, which was evaluated at 3 and 6 days after treatment initiation, could have missed the time of maximally detectable treatment induced-cell death.

AKT activation stimulates glucose import and metabolism (33), and most glycolytic enzyme genes are transcriptionally regulated by AKT and mTOR signaling (34). To evaluate the effects of Tz and rapamycin on glucose metabolism, we measured [^{18}F]FDG uptake by positron emission tomography (PET). Baseline tumor [^{18}F]FDG uptake was determined, then mice were randomized to drug treatment on days 0, 2, 4, and 6, and re-imaged on days 3 and 7. While the single-agent treatments induced an apparent trend towards decreased [^{18}F]FDG tumor uptake, these groups were not significantly different from controls (Fig. 4B). However, the combination treatment induced a strong trend towards decreased [^{18}F]FDG tumor uptake compared to controls after 7 days ($p=0.0586$, Fig. 4B); significant changes were not observed on day 3 (not shown). A separate set of tumor-bearing mice were treated on days 0, 2, and 5, and tumors were harvested on day 6 for immunoblot analysis. Tumors from combination-treated mice showed decreased levels of several signaling proteins [HER3, HER2, insulin

receptor substrate-1 (IRS-1); Fig. S3]. Therefore, the decreased [^{18}F]FDG tumor uptake at day 7 may have been linked to cell death, in agreement with the decrease in tumor size seen after 0.5 weeks of combination treatment (Fig. 2).

mTOR inhibitor RAD001 synergizes with trastuzumab to inhibit HER2+ breast cancer cell growth

To determine whether mTOR inhibition directly potentiates the effects of Tz in a tumor cell-autonomous manner, we evaluated the effects of the combination on the proliferation of SKBR3 and BT474 cells. Both lines harbor *HER2* gene amplification and wild-type *PTEN*. SKBR3 cells have wild type *PIK3CA*, whereas BT474 carry a weakly transforming *PIK3CA* mutation (35). While treatment with Tz or the mTOR inhibitor RAD001 alone significantly inhibited BT474 and SKBR3 cell proliferation (Fig. 5A), the combination was significantly more effective than either agent alone (all $p<0.005$). However, the combination only marginally increased apoptosis in BT474 cells after three days compared to control or Tz-treated cells (3.41%, 2.15%, and 2.1%, respectively; Fig. S4). Therefore, Tz and RAD001 appear to have a primarily cytostatic effect in culture.

We then analyzed the effects of Tz and RAD001 on HER2 and mTOR signaling *in vitro*. While Tz treatment had only a modest inhibitory effect on mTOR activity (indicated by P-S6 levels), RAD001 completely blocked it (Fig. 5B). In agreement with prior findings (12,36,37), Tz partially decreased P-AKT, indicating partial inhibition of PI3K signaling. P-HER3 activates PI3K, and HER3 function is required for the transforming effects of overexpressed HER2 (38). In agreement with our prior observations (12), the Tz-induced inhibition of PI3K is associated with decreased P-HER3, supporting the notion that HER2 primarily transactivates HER3 in HER2+ cells. Inhibition of mTOR has been shown to activate the insulin-like growth factor-I receptor (IGF-IR)/IRS-1 (39) and MAPK (40) pathways through derepression of negative feedback loops. Here, RAD001 treatment increased P-AKT$_{S473}$, P-AKT$_{T308}$, P-MAPK, and P-HER3 but did not alter IRS-1 levels (Figs. 5B, 5D). These RAD001-induced effects were partially blocked by co-treatment with Tz (Fig. 5B), suggesting that feedback to activate HER3, PI3K, and MAPK was partially dependent on HER2. These results suggest that the combination of Tz plus RAD001 simultaneously suppresses both PI3K and mTOR signaling which, in turn, contributes to their synergistic inhibition of cell proliferation

We further evaluated the ability of RAD001 to overcome Tz-resistant growth in HR5 and HR6 cell lines, which were derived from BT474 xenografts with acquired Tz resistance *in vivo* (15). Compared to parental, Tz-sensitive BT474 cells, both resistant lines exhibited higher basal levels of P-S6, which were not altered by Tz treatment. Treatment with RAD001, but not Tz, significantly inhibited HR5/6 cell growth (Fig. 5E-F), suggesting that mTOR inhibition may be an effective therapeutic strategy against Tz-resistant breast cancers.

Since HER2-mediated AKT activation is partially suppressed by Tz, but RAD001 treatment increased P-AKT (Fig. 5B), we assessed whether direct inhibition of AKT could synergize with mTOR inhibition to suppress cell proliferation. Indeed, treatment with RAD001 or an AKT1/2 inhibitor (AKTi) significantly inhibited cell proliferation, and the combination was more effective than either agent alone (Fig. 5C, all $p<0.01$). While AKTi only modestly decreased PS6, RAD001 completely blocked it (Fig. 5D). RAD001 increased P-AKT and P-MAPK, and cotreatment with AKTi partially abrogated P-AKT but further increased P-MAPK.

The above data imply that Tz is unable to inhibit mTOR. mTOR inhibition results in AKT activation, and counteracting this activation with Tz or the AKT inhibitor improves response to treatment. These findings collectively suggest that mTOR signaling promotes resistance to HER2 inhibitors. To test this, we used siRNA to knockdown *Tuberous sclerosis 2* (*TSC2*) expression, thus derepressing Rheb to activate mTOR (Fig. 6A-B). The EGFR/HER2 dual

kinase inhibitor lapatinib potently inhibits PI3K signaling in HER2+ cancer cell lines (41). While lapatinib treatment effectively decreased P-HER2, P-HER3, P-AKT, P-MAPK, and P-S6 levels, P-S6 remained higher in siTSC2 cells compared to siCtl, indicating HER2-independent activation of mTOR. RAD001 treatment completely inhibited P-S6, and the combination of lapatinib plus RAD001 completely blocked both P-S6 and P-AKT. We found that *TSC2* knockdown attenuated lapatinib-induced growth inhibition (Fig. 6C-D), further implying an association between the decoupling of mTOR from HER2 upstream and the relative resistance to lapatinib. The shift in the degree of response to lapatinib conferred by *TSC2* knockdown was abrogated by RAD001 treatment, further implying that the increased growth of siTSC2 cells in the presence of the HER2 inhibitor was due to mTOR signaling. Notably, Tz, lapatinib, and AKTi decreased P-AKT (Figs. 5B, 5D, 6A-B) but did not completely block P-S6, suggesting that blocking mTOR by inhibiting upstream signaling components may be less effective than inhibiting mTOR directly. These results collectively suggest that blockade of mTOR is required for the full antitumor effect of HER2 inhibitors.

Discussion

Herein, we demonstrate the complete regression of HER2-overexpressing tumors using the combination of Tz and rapamycin. Treatment with the combination promptly induced tumor cell death within 1.5 days as detected by non-invasive imaging. These findings support the clinical exploration of combined Tz and mTOR inhibitor therapies for the treatment of HER2 + breast cancer, and the use of non-invasive imaging approaches that detect tumor cell apoptosis (like Annexin-V imaging) to detect early response to therapy.

The anti-tumor mechanism(s) of Tz action in patients with HER2+ tumors remains unclear. Tz is thought to mediate antibody-dependent cellular cytotoxicity by binding Fcγ receptor III (10,42). One week of neoadjuvant Tz therapy increased apoptosis in HER2+ human breast cancers with no significant effect on Ki67 immunoreactivity (9). We previously found that two to three weeks of Tz treatment also increased apoptosis in MMTV/HER2 tumors, but cell proliferation was unaffected (31). Herein, the combination of Tz plus rapamycin significantly increased NIR700-Annexin-V tumor uptake as assessed by non-invasive imaging at 40 h after a single dose, suggesting rapid induction of cell death. In contrast, Tz induces a cytostatic effect on cultured HER2+ cancer cells without inducing apoptosis [Figs. 5A and S4, and (11)].

While Tz treatment did not alter MMTV/HER2 tumor cell proliferation *in vivo*, rapamycin treatment drastically decreased both P-S6 levels and Ki67 immunoreactivity after only three days (Fig. 3). Mosley *et al*. observed similar effects of rapamycin on mammary tumors in MMTV/Neu transgenic female mice, which express the rat homologue of *HER2* (43). mTOR is a critical signaling hub in the PI3K/AKT pathway. Consistent with this, rapamycin inhibits the growth of tumor cells with oncogenic mutations in *AKT* or deletion of the tumor suppressor *PTEN* [reviewed in (44)]. We therefore speculate that mTOR inhibition blocks cell proliferation to potentiate Tz effects. Interestingly, the potential immunosuppressive effects of rapamycin (45), if they occurred in our model, did not block the antitumor effect of Tz. Therefore, if Tz utilized an immune mechanism to induce tumor regression, this action was not appreciably affected by rapamycin. Additionally, rapamycin can have anti-angiogenic effects on tumor vasculature, and decrease tumor blood vessel permeability (23). Although we found that the combination of Tz plus rapamycin induced significant tumor regression after 0.5 weeks (Fig. 2), we did not observe changes in tumor vasculature after 3 or 6 days of single or combined drug treatments (as assessed by H&E staining and CD31 IHC). Our results are in agreement with a previous report on rapamycin treatment of mice bearing MMTV/Neu tumors (43).

Inhibition of mTOR has been shown to upregulate PI3K signaling to activate the AKT (39) and Ras/MAPK (40) pathways through derepression of feedback loops. Similarly, we observed RAD001-induced increases in P-AKT and P-MAPK in BT474 and SKBR3 cells *in vitro*, which may be related to an increase in P-HER3 (Figs. 5-6). The reason that these effects were not observed in MMTV/HER2 tumors upon rapamycin treatment will require further study (Figs. 3C & S3). While O'Reilly *et al*. found that inhibition of mTOR increased P-AKT in MCF-7 and DU-145 cancer cells via an IGF-IR/IRS-1-dependent mechanism (39), we observed RAD001-induced upregulation of P-HER3 but not IRS-1 in BT474 and SKBR3 cells (Fig. 5). Since Tz inhibited the RAD001-induced increases in P-HER3 and P-AKT, we deduce that mTOR inhibition increased PI3K signaling via HER2-activated HER3. We speculate that cells upregulate intact mechanisms of PI3K activation when confronted with mTOR inhibition [via HER3 in HER2+ BT474 and SKBR3 cells (Fig. 5), and via IRS-1 in HER2-low MCF-7 and DU-145 cells (39)].

mTOR inhibitors have been shown to synergize with receptor tyrosine kinase inhibitors. Treatment of cancer cells with the EGFR inhibitor erlotinib or an IGF-1R inhibitor blocked rapamycin-induced increases in P-AKT, and drug combinations were more effective than single-agent treatments at inhibiting cell growth (46). RAD001 combined with the EGFR inhibitor gefitinib more effectively slowed the growth of human GEO colon cancer xenografts in nude mice than either drug alone (47). Similarly, we showed that mTOR inhibitors combined with either Tz or an AKT inhibitor were more effective than any single agent. Tz plus RAD001 simultaneously suppressed PI3K and mTOR signaling, as shown by reduced P-AKT and P-S6 levels (Fig. 5). In contrast, lapatinib plus RAD001 was only slightly more effective than lapatinib alone in BT474 cells, and not in SKBR3 cells (Fig. 6). This may be related to the ability of lapatinib to potently inhibit P-AKT and, in turn, significantly reduce mTOR activity. These effects were partially abrogated by *TSC2* knockdown, which conferred HER2-independent activation of mTOR. These findings collectively highlight the need to completely block both PI3K/AKT and mTOR for maximal action of anti-HER2 therapies.

We found that Tz plus rapamycin induced complete regression of all MMTV/HER2 tumors (Fig. 2). In contrast, Lu *et al*. reported that treatment of severe-combined immunodeficiency mice bearing BT474 xenografts with Tz, RAD001, or the combination did not significantly affect tumor growth, although the combination showed an inhibitory trend (21). However, Lu *et al*. used suboptimal doses of 0.5 mg/kg Tz twice weekly [effective doses in mice are 10-30 mg/kg 2x/week (27,48)]. Our conflicting observations may be attributable to differences between experimental systems, including the drugs, doses, routes of administration, tumor types, and immune competence of each animal model. For example, although BT474 xenografts in nude mice are initially sensitive to Tz treatment, we found that tumors became resistant after five weeks (15). Given the emerging importance of the immunological role of Tz in its anti-tumor action (10), we cannot rule out that the synergistic effects of Tz and rapamycin seen in the MMTV/HER2 model depend on an intact host immune system.

HER2+ human breast tumors showed increased caspase-3 activation by IHC after one week of Tz therapy (9). Obtaining patient tumor tissue through serial biopsy is invasive and clinically impractical to routinely assess treatment response. Alternatively, non-invasive molecular imaging biomarkers such as Annexin-V binding and [^{18}F]FDG uptake could be valuable for clinical prediction of treatment response. We previously demonstrated that NIR700-Annexin-V imaging correlated with tumor cell apoptosis and predicted outcome following Tz therapy in MMTV/HER2 tumor-bearing mice (31). Since treatment with the combination of Tz plus rapamycin induced significant tumor regression after 0.5 weeks (Fig. 2), we analyzed early induction of cell death by Annexin-V imaging after a single treatment in each of the arms. Only the combination significantly increased tumor Annexin-V uptake compared to controls (Fig. 4A). Since all tumors treated with the combination ultimately regressed completely, Annexin-

V imaging was strongly predictive of outcome in this model. We also observed a trend towards decreased [^{18}F]FDG uptake after one week of combination treatment. IHC analysis of cleaved caspase-3 and H&E staining after three and six days of treatment showed widespread areas of necrosis in all groups, precluding quantification of apoptotic cells. The detection of changes in cell death by conventional IHC may be further complicated by heterogeneity between tumors, which can be circumvented by serial, non-invasive imaging of the same subjects pre- and post-treatment (Fig. 4). Our data support further exploration of the clinical potential of Annexin-V and [^{18}F]FDG imaging as non-invasive tools to assess early response to therapy.

In conclusion, our findings support the ongoing clinical evaluation of drug combinations simultaneously targeting both HER2 and mTOR. Early results from a phase I trial in patients with Tz-resistant breast cancer showed that the combination of Tz, RAD001, and paclitaxel induced a partial response (PR) in 5/7 patients, minor regression in 1 patient, stable disease (SD) in another, and prevented progression of disease (PD) in 11/13 patients who continued treatment (24). In another phase I trial testing the combination of Tz, RAD001, and vinorelbine in 22 heavily pretreated breast cancer patients, 1 had complete response (CR), 2 had PR, 15 had SD, and 4 had PD, yielding a clinical benefit rate (CR+PR+SD>24 weeks) of 55% (25). Since mTOR is a critical PI3K pathway effector and mutational activation of the PI3K pathway has been clinically associated with Tz resistance (13,14), our findings suggest that combined treatment with an mTOR inhibitor should be an effective therapeutic strategy to combat Tz-resistant, HER2+ cancer.

Statement of Translational Relevance

While trastuzumab therapy has significantly improved outcome for patients with advanced HER2-positive breast cancer, a fraction of these cancers exhibit *de novo* or acquired resistance. Activation of the phosphatidylinositol-3 kinase (PI3K) signaling pathway has been linked with trastuzumab resistance, making this pathway a therapeutic target of interest. The mTORC1 serine/threonine kinase complex is a major effector in the PI3K pathway, and mTOR inhibitors suppress cancer cell growth in various model systems. We demonstrate that mTOR inhibitors synergize with Trastuzumab to induce complete regression of HER2-positive mouse mammary tumors *in vivo*, and to suppress the growth of HER2-positive human breast cancer cells *in vitro*. These findings support the use of combinations of trastuzumab and mTOR inhibitors for the treatment of patients with HER2 + breast cancer.

Supplementary Material

Refer to Web version on PubMed Central for supplementary material.

Acknowledgments

Funding: This work was supported by NIH R01CA80195 (C.L.A.), F32CA121900 (T.W.M.), K25CA127349 (H.C.M.), Breast Cancer Specialized Program of Research Excellence (SPORE) P50CA98131, South-Eastern Center for Small-Animal Imaging U24CA126588 (H.C.M.), S.K.W. is supported by T32EB001628; Vanderbilt-Ingram Comprehensive Cancer Center Support Grant P30CA68485; ACS Clinical Research Professorship Grant CRP-07-234 (C.L.A.); American Cancer Society [IRG-58-009-49 (C.W.L.)]

References

1. Slamon DJ, Clark GM, Wong SG, Levin WJ, Ullrich A, McGuire WL. Human breast cancer: correlation of relapse and survival with amplification of the HER-2/neu oncogene. Science 1987;235:177–82. [PubMed: 3798106]

2. Slamon DJ, Godolphin W, Jones LA, et al. Studies of the HER-2/neu proto-oncogene in human breast and ovarian cancer. Science 1989;244:707–12. [PubMed: 2470152]
3. Carter P, Presta L, Gorman CM, et al. Humanization of an anti-p185HER2 antibody for human cancer therapy. Proc Natl Acad Sci U S A 1992;89:4285–9. [PubMed: 1350088]
4. Baselga J, Tripathy D, Mendelsohn J, et al. Phase II study of weekly intravenous recombinant humanized anti-p185HER2 monoclonal antibody in patients with HER2/neu-overexpressing metastatic breast cancer. J Clin Oncol 1996;14:737–44. [PubMed: 8622019]
5. Cobleigh MA, Vogel CL, Tripathy D, et al. Multinational study of the efficacy and safety of humanized anti-HER2 monoclonal antibody in women who have HER2-overexpressing metastatic breast cancer that has progressed after chemotherapy for metastatic disease. J Clin Oncol 1999;17:2639–48. [PubMed: 10561337]
6. Piccart-Gebhart MJ, Procter M, Leyland-Jones B, et al. Trastuzumab after adjuvant chemotherapy in HER2-positive breast cancer. N Engl J Med 2005;353:1659–72. [PubMed: 16236737]
7. Romond EH, Perez EA, Bryant J, et al. Trastuzumab plus adjuvant chemotherapy for operable HER2-positive breast cancer. N Engl J Med 2005;353:1673–84. [PubMed: 16236738]
8. Slamon DJ, Leyland-Jones B, Shak S, et al. Use of chemotherapy plus a monoclonal antibody against HER2 for metastatic breast cancer that overexpresses HER2. N Engl J Med 2001;344:783–92. [PubMed: 11248153]
9. Mohsin SK, Weiss HL, Gutierrez MC, et al. Neoadjuvant trastuzumab induces apoptosis in primary breast cancers. J Clin Oncol 2005;23:2460–8. [PubMed: 15710948]
10. Musolino A, Naldi N, Bortesi B, et al. Immunoglobulin G fragment C receptor polymorphisms and clinical efficacy of trastuzumab-based therapy in patients with HER-2/neu-positive metastatic breast cancer. J Clin Oncol 2008;26:1789–96. [PubMed: 18347005]
11. Pegram M, Hsu S, Lewis G, et al. Inhibitory effects of combinations of HER-2/neu antibody and chemotherapeutic agents used for treatment of human breast cancers. Oncogene 1999;18:2241–51. [PubMed: 10327070]
12. Yakes FM, Chinratanalab W, Ritter CA, King W, Seelig S, Arteaga CL. Herceptin-induced inhibition of phosphatidylinositol-3 kinase and Akt Is required for antibody-mediated effects on p27, cyclin D1, and antitumor action. Cancer Res 2002;62:4132–41. [PubMed: 12124352]
13. Berns K, Horlings HM, Hennessy BT, et al. A functional genetic approach identifies the PI3K pathway as a major determinant of trastuzumab resistance in breast cancer. Cancer Cell 2007;12:395–402. [PubMed: 17936563]
14. Nagata Y, Lan KH, Zhou X, et al. PTEN activation contributes to tumor inhibition by trastuzumab, and loss of PTEN predicts trastuzumab resistance in patients. Cancer Cell 2004;6:117–27. [PubMed: 15324695]
15. Ritter CA, Perez-Torres M, Rinehart C, et al. Human breast cancer cells selected for resistance to trastuzumab in vivo overexpress epidermal growth factor receptor and ErbB ligands and remain dependent on the ErbB receptor network. Clin Cancer Res 2007;13:4909–19. [PubMed: 17699871]
16. Rosen N, She QB. AKT and cancer--is it all mTOR? Cancer Cell 2006;10:254–6. [PubMed: 17045203]
17. Fan QW, Cheng C, Knight ZA, et al. EGFR signals to mTOR through PKC and independently of Akt in glioma. Sci Signal 2009;2:ra4. [PubMed: 19176518]
18. Awada A, Cardoso F, Fontaine C, et al. The oral mTOR inhibitor RAD001 (everolimus) in combination with letrozole in patients with advanced breast cancer: results of a phase I study with pharmacokinetics. Eur J Cancer 2008;44:84–91. [PubMed: 18039566]
19. Motzer RJ, Escudier B, Oudard S, et al. Efficacy of everolimus in advanced renal cell carcinoma: a double-blind, randomised, placebo-controlled phase III trial. Lancet 2008;372:449–56. [PubMed: 18653228]
20. Squarize CH, Castilho RM, Gutkind JS. Chemoprevention and treatment of experimental Cowden's disease by mTOR inhibition with rapamycin. Cancer Res 2008;68:7066–72. [PubMed: 18757421]
21. Lu CH, Wyszomierski SL, Tseng LM, et al. Preclinical testing of clinically applicable strategies for overcoming trastuzumab resistance caused by PTEN deficiency. Clin Cancer Res 2007;13:5883–8. [PubMed: 17908983]

22. Price DJ, Grove JR, Calvo V, Avruch J, Bierer BE. Rapamycin-induced inhibition of the 70-kilodalton S6 protein kinase. Science 1992;257:973–7. [PubMed: 1380182]
23. Phung TL, Ziv K, Dabydeen D, et al. Pathological angiogenesis is induced by sustained Akt signaling and inhibited by rapamycin. Cancer Cell 2006;10:159–70. [PubMed: 16904613]
24. André F, Campone M, Hurvitz SA, Vittori L, Pylvaenaeinen I, Sahmoud T, O'Regan RM. Multicenter phase I clinical trial of daily and weekly RAD001 in combination with weekly paclitaxel and trastuzumab in patients with HER2-overexpressing metastatic breast cancer with prior resistance to trastuzumab. Journal of Clinical Oncology 2008;26Abstract 1003
25. Fasolo, A.; Gianni, L.; Rorive, A.; Bergh, J.; Dieras, V.; Cardoso, F.; Vittori, L.; Pylvaenaeinen, I.; Sahmoud, T.; Jerusalem, G. Multicenter phase I clinical trial of daily and weekly RAD001 (everolimus) in combination with vinorelbine and trastuzumab in patients with HER-2-overexpressing metastatic breast cancer with prior resistance to trastuzumab. San Antonio Breast Cancer Symposium; 2008; 2008. Abstract # 406
26. Finkle D, Quan ZR, Asghari V, et al. HER2-targeted therapy reduces incidence and progression of midlife mammary tumors in female murine mammary tumor virus huHER2-transgenic mice. Clin Cancer Res 2004;10:2499–511. [PubMed: 15073130]
27. Reyzer ML, Caldwell RL, Dugger TC, et al. Early changes in protein expression detected by mass spectrometry predict tumor response to molecular therapeutics. Cancer Res 2004;64:9093–100. [PubMed: 15604278]
28. Guix M, Faber AC, Wang SE, et al. Acquired resistance to EGFR tyrosine kinase inhibitors in cancer cells is mediated by loss of IGF-binding proteins. J Clin Invest 2008;118:2609–19. [PubMed: 18568074]
29. Schuler W, Sedrani R, Cottens S, et al. SDZ RAD, a new rapamycin derivative: pharmacological properties in vitro and in vivo. Transplantation 1997;64:36–42. [PubMed: 9233698]
30. Lindsley CW, Zhao Z, Leister WH, et al. Allosteric Akt (PKB) inhibitors: discovery and SAR of isozyme selective inhibitors. Bioorg Med Chem Lett 2005;15:761–4. [PubMed: 15664853]
31. Shah C, Miller TW, Wyatt SK, et al. Imaging biomarkers predict response to anti-HER2 (ErbB2) therapy in preclinical models of breast cancer. Clin Cancer Res 2009;15:4712–21. [PubMed: 19584166]
32. Chung J, Kuo CJ, Crabtree GR, Blenis J. Rapamycin-FKBP specifically blocks growth-dependent activation of and signaling by the 70 kd S6 protein kinases. Cell 1992;69:1227–36. [PubMed: 1377606]
33. Plas DR, Thompson CB. Akt-dependent transformation: there is more to growth than just surviving. Oncogene 2005;24:7435–42. [PubMed: 16288290]
34. Majumder PK, Febbo PG, Bikoff R, et al. mTOR inhibition reverses Akt-dependent prostate intraepithelial neoplasia through regulation of apoptotic and HIF-1-dependent pathways. Nat Med 2004;10:594–601. [PubMed: 15156201]
35. Saal LH, Holm K, Maurer M, et al. PIK3CA mutations correlate with hormone receptors, node metastasis, and ERBB2, and are mutually exclusive with PTEN loss in human breast carcinoma. Cancer Res 2005;65:2554–9. [PubMed: 15805248]
36. Lane HA, Beuvink I, Motoyama AB, Daly JM, Neve RM, Hynes NE. ErbB2 potentiates breast tumor proliferation through modulation of p27(Kip1)-Cdk2 complex formation: receptor overexpression does not determine growth dependency. Mol Cell Biol 2000;20:3210–23. [PubMed: 10757805]
37. Lee H, Akita RW, Sliwkowski MX, Maihle NJ. A naturally occurring secreted human ErbB3 receptor isoform inhibits heregulin-stimulated activation of ErbB2, ErbB3, and ErbB4. Cancer Res 2001;61:4467–73. [PubMed: 11389077]
38. Lee-Hoeflich ST, Crocker L, Yao E, et al. A central role for HER3 in HER2-amplified breast cancer: implications for targeted therapy. Cancer Res 2008;68:5878–87. [PubMed: 18632642]
39. O'Reilly KE, Rojo F, She QB, et al. mTOR inhibition induces upstream receptor tyrosine kinase signaling and activates Akt. Cancer Res 2006;66:1500–8. [PubMed: 16452206]
40. Carracedo A, Ma L, Teruya-Feldstein J, et al. Inhibition of mTORC1 leads to MAPK pathway activation through a PI3K-dependent feedback loop in human cancer. J Clin Invest 2008;118:3065–74. [PubMed: 18725988]

41. Konecny GE, Pegram MD, Venkatesan N, et al. Activity of the dual kinase inhibitor lapatinib (GW572016) against HER-2-overexpressing and trastuzumab-treated breast cancer cells. Cancer Res 2006;66:1630–9. [PubMed: 16452222]

42. Clynes RA, Towers TL, Presta LG, Ravetch JV. Inhibitory Fc receptors modulate in vivo cytoxicity against tumor targets. Nat Med 2000;6:443–6. [PubMed: 10742152]

43. Mosley JD, Poirier JT, Seachrist DD, Landis MD, Keri RA. Rapamycin inhibits multiple stages of c-Neu/ErbB2 induced tumor progression in a transgenic mouse model of HER2-positive breast cancer. Mol Cancer Ther 2007;6:2188–97. [PubMed: 17699716]

44. Guertin DA, Sabatini DM. Defining the role of mTOR in cancer. Cancer Cell 2007;12:9–22. [PubMed: 17613433]

45. Gutierrez-Dalmau A, Campistol JM. Immunosuppressive therapy and malignancy in organ transplant recipients: a systematic review. Drugs 2007;67:1167–98. [PubMed: 17521218]

46. Buck E, Eyzaguirre A, Brown E, et al. Rapamycin synergizes with the epidermal growth factor receptor inhibitor erlotinib in non-small-cell lung, pancreatic, colon, and breast tumors. Mol Cancer Ther 2006;5:2676–84. [PubMed: 17121914]

47. Bianco R, Garofalo S, Rosa R, et al. Inhibition of mTOR pathway by everolimus cooperates with EGFR inhibitors in human tumours sensitive and resistant to anti-EGFR drugs. Br J Cancer 2008;98:923–30. [PubMed: 18319715]

48. Baselga J, Norton L, Albanell J, Kim YM, Mendelsohn J. Recombinant humanized anti-HER2 antibody (Herceptin) enhances the antitumor activity of paclitaxel and doxorubicin against HER2/neu overexpressing human breast cancer xenografts. Cancer Res 1998;58:2825–31. [PubMed: 9661897]

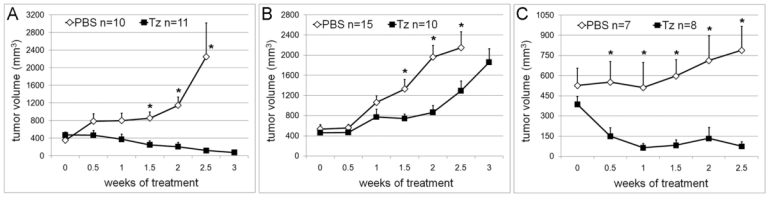

Fig. 1.

Trastuzumab inhibits MMTV/HER2 tumor growth. Three groups of mice (A, B, and C) bearing MMTV/HER2 tumors derived from three transgenic donors were randomized to Tz or PBS when tumor volume reached ≥200 mm^3. Average volume ± SEM is shown. *p<0.05 by Mann-Whitney U-test comparing Tz and PBS groups at each time point.

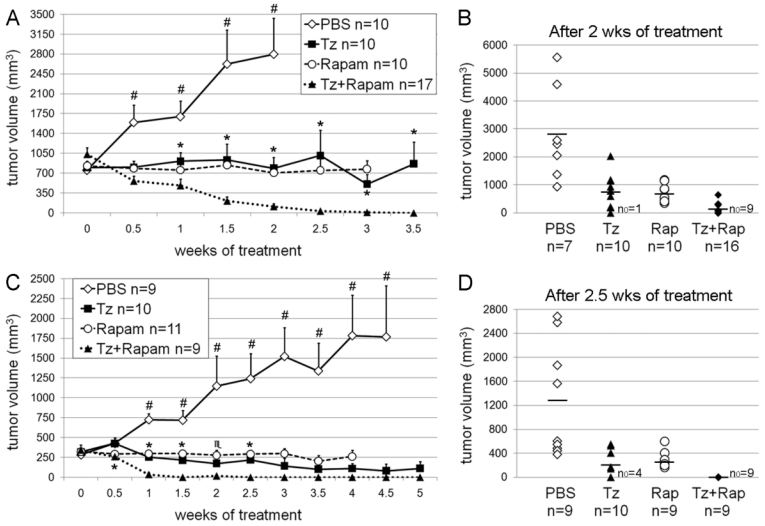

Fig. 2.

Rapamycin synergizes with trastuzumab to induce complete tumor regression. Two groups of MMTV/HER2 tumor-bearing mice (D and E) were randomized to Tz, rapamycin, or the combination once tumor volume reached ≥400 mm^3 (A,B) or ≥200 mm^3 (C,D). A,C) Average volume ± SEM is shown. *$p<0.05$, ℳ$p=0.052$ by Mann-Whitney U-test comparing Tz and combination groups at each time point. #$p<0.05$ by all three Mann-Whitney U-tests comparing vehicle with each other treatment group. B,D) Tumor volume for each mouse after 2.5 weeks (B shows group D) and 2 weeks (D shows group E) of treatment is shown. Bars indicate average volumes. n_0 = number of mice with tumors that completely regressed. Numbers of animals decreased slightly at later time points due to excessive tumor burden.

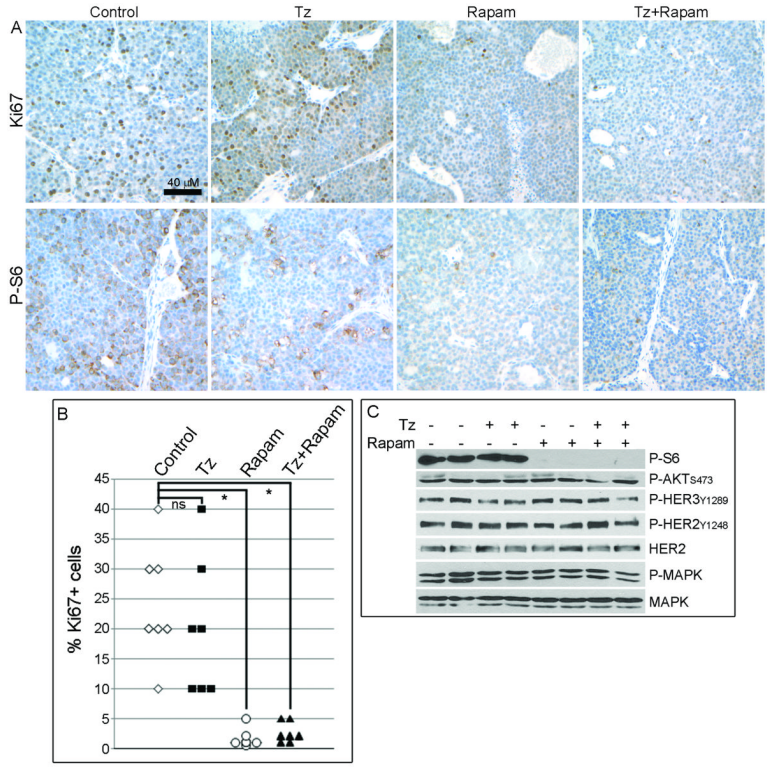

Fig. 3.

Rapamycin inhibits mTOR and tumor cell proliferation. Tumor-bearing mice were treated with Tz, rapamycin, or the combination (n=6-7 per group) on days 0 and 2, and tumors were harvested 24 h later. A) IHC analysis of Ki67 (*top row*) and P-S6 (*bottom row*) in tumor sections. B) Quantitative comparison of % Ki67+ tumor cells from (A). **p*<0.005 by Mann-Whitney U-test comparing control with each treatment group. ns- not significant. C) Immunoblot analysis of lysates from tumors used in (A). Each lane contains equal amounts of protein pooled from 3-4 tumors. Blots were probed with indicated antibodies.

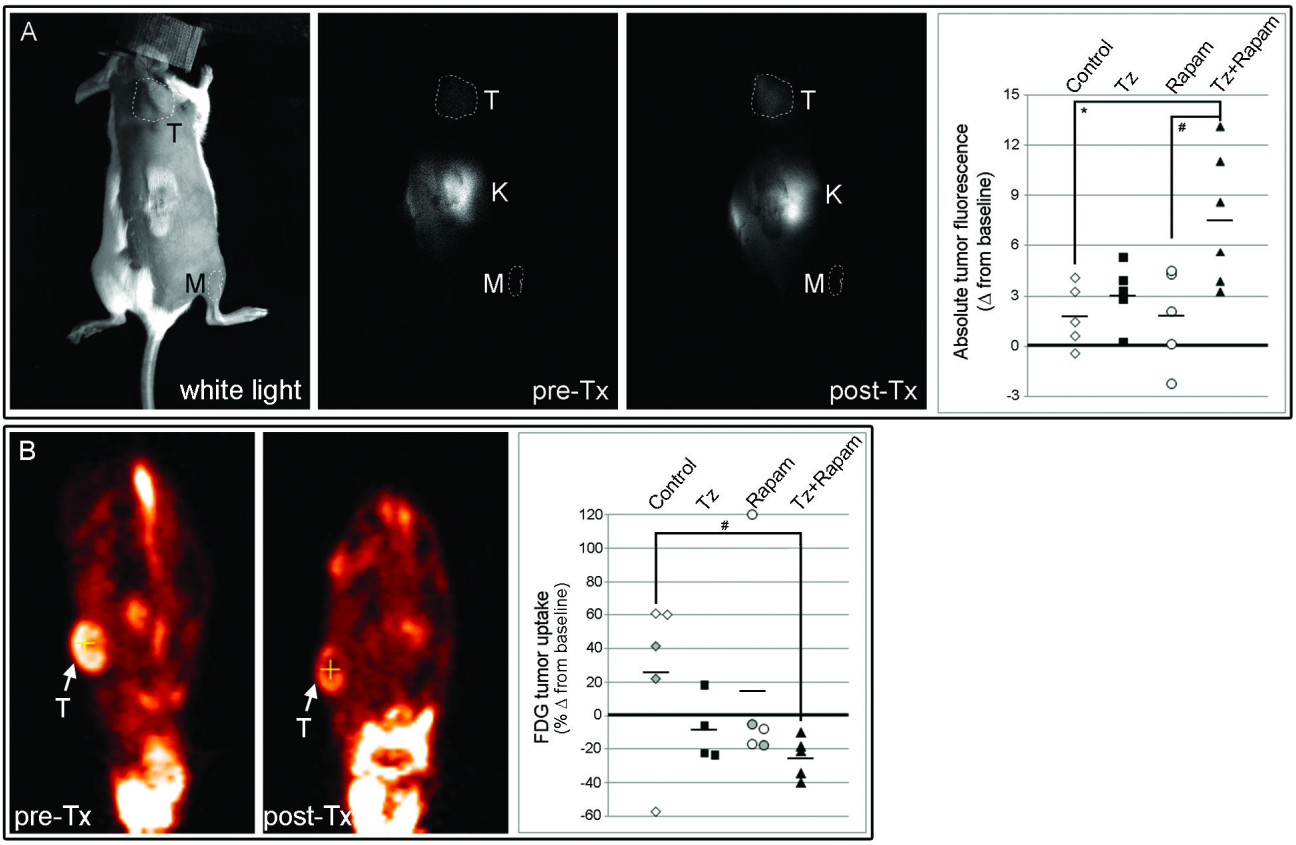

Fig. 4.

Rapamycin synergizes with trastuzumab to decrease tumor viability and glucose metabolism. A) Tumor-bearing mice were imaged at baseline using NIR700-Annexin-V, then randomized to Tz, rapamycin, or the combination (n=5-6 per group), and re-imaged 40 h post-treatment. Representative image shows tumor location (white light) and NIR700-Annexin-V signals at pre- and post-treatment. T=tumor; M=hindlimb reference muscle (internal control); K=kidney (Annexin-V is cleared via kidney). Plot of the change in absolute tumor fluorescence (ATF) induced by drug treatment for each mouse is shown at right. Bars indicate group averages. $^{*}p<0.05$, $^{\#}p=0.052$ by Mann-Whitney U-test between treatment groups. B) Tumor-bearing mice were baseline imaged by PET for [^{18}F]FDG uptake, treated as above on days 0, 2, 4, and 6, and re-imaged on day 7 (n=4-5 per group). Images from a representative mouse show [^{18}F]FDG uptake pre- and post-treatment. Plot of the % change in [^{18}F]FDG uptake at day 7 compared to baseline is shown at right. Gray diamonds/circles are indicative of two tumors within the same mouse. $^{\#}p=0.0586$ by Mann-Whitney U-test between treatment groups.

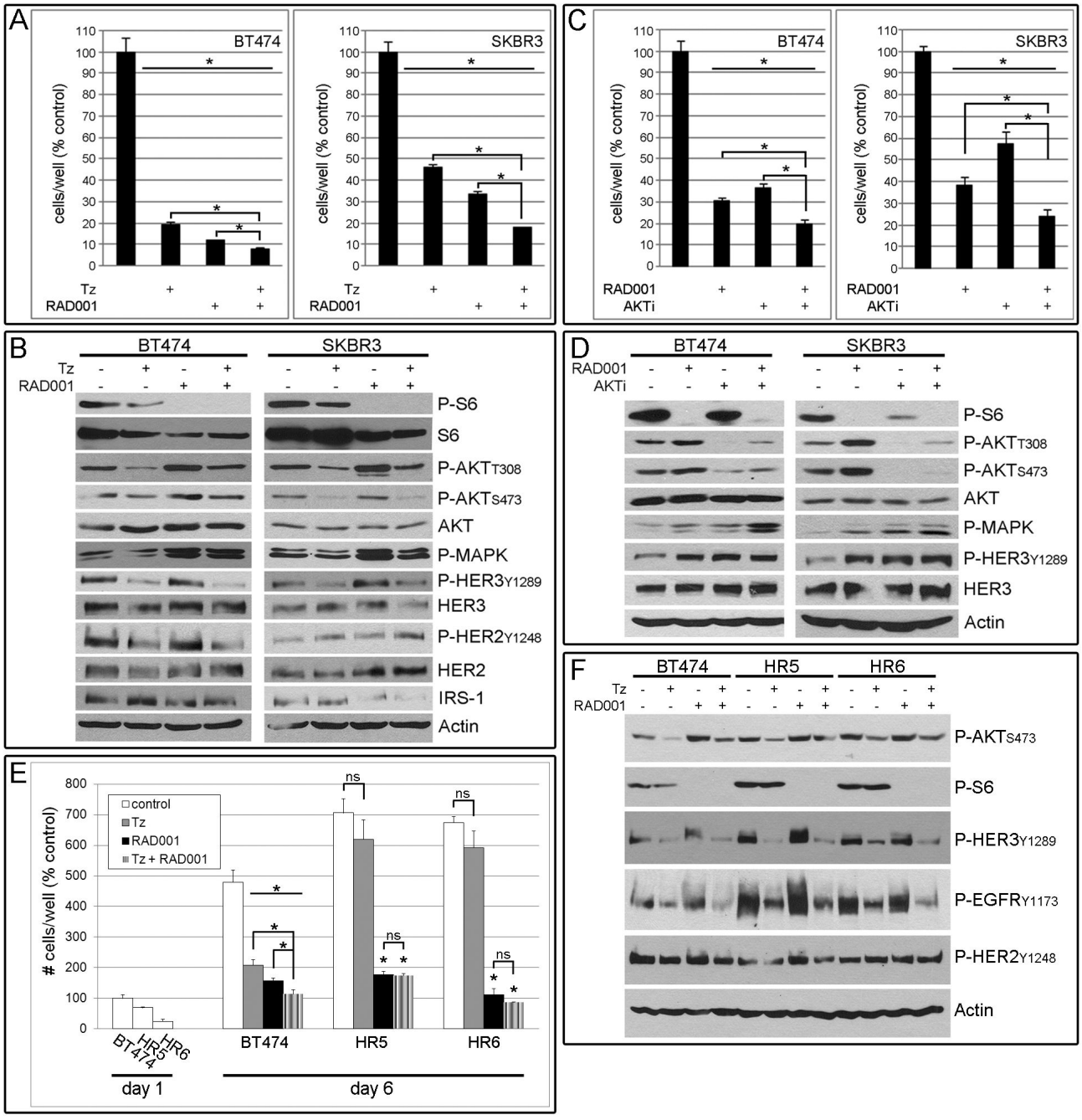

Fig. 5.

RAD001 synergizes with trastuzumab to inhibit HER2+ breast cancer cell growth. A) BT474 and SKBR3 cells were treated ± Tz, RAD001, or the combination in their respective growth media. Cells were counted after 6-7 days [presented as mean of triplicates ± SD (% control)]. **p*<0.005 by *t*-test. B) Immunoblot analysis of cells treated ± Tz and RAD001 under serum-free conditions for 24 h. Blots were probed with indicated antibodies. C) BT474 and SKBR3 cells were treated ± RAD001, AKTi, or both. Cells were analyzed as in (A). **p*<0.01. D) Immunoblot analysis of cells treated ± RAD001 and AKTi under serum-free conditions for 24 hrs. E) BT474, HR5, and HR6 cells were treated as in (A), and counted after 1 or 6 days. **p*<0.05. F) Immunoblot analysis of cells treated as in (B).

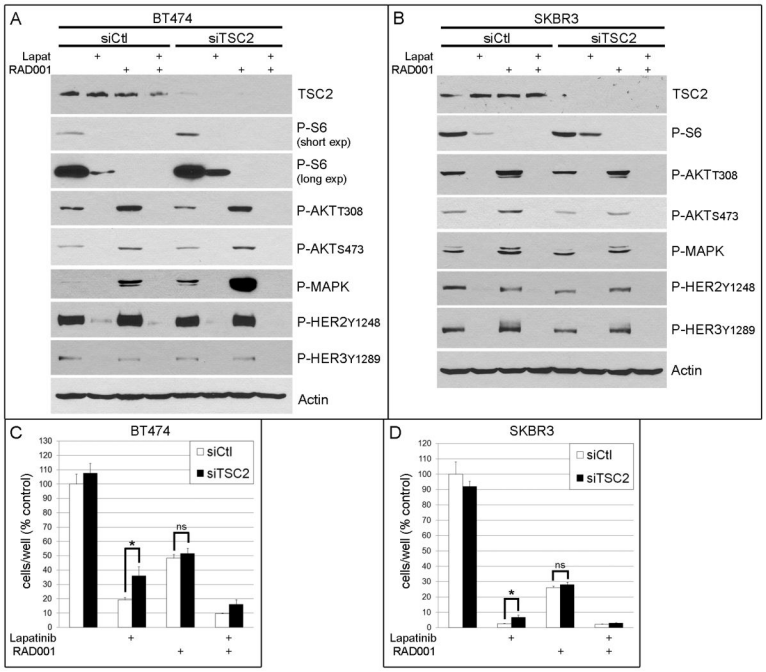

Fig. 6.

Constitutive mTOR signaling attenuates response to lapatinib in HER2+ breast cancer cells. A-B) Immunoblot analysis of BT474 (A) and SKBR3 (B) cells transfected with siRNA against *TSC2* or control (siCtl), then treated ± lapatinib, RAD001, or both under serum-free conditions for 24 h. Blots were probed with indicated antibodies. C-D) Proliferation assays of cells treated as in (A-B) in growth media. Cells were counted after 6-7 days [presented as mean of triplicates ± SD (% control)]. **p*<0.05 by *t*-test. ns- not significant.